QUALITATIVE STUDY ON THE EFFECT OF SLAG COMPOSITION ON THE PYROMETALLURGICAL RECYCLING OF LITHIUM-ION BATTERY BLACK MASS

[1]Safoura BABANEJAD, [2]Hesham AHMED, [3]Charlotte ANDERSSON

[1]Department of Civil, Environmental and Natural Resource Engineering, Process Metallurgy, Minerals and Metallurgical Engineering, Luleå University of Technology, 971 87 Luleå, Sweden, safbab@ltu.se

[2]Department of Civil, Environmental and Natural Resource Engineering, Process Metallurgy, Minerals and Metallurgical Engineering, Luleå University of Technology, 971 87 Luleå, Sweden, hesham.ahmed@ltu.se

[2]Central Metallurgical Research and Development Institute, P.O. Box 87, Helwan 114 21, Egypt

[3]Department of Civil, Environmental and Natural Resource Engineering, Process Metallurgy, Minerals and Metallurgical Engineering, Luleå University of Technology, 971 87 Luleå, Sweden, charlotte.andersson@ltu.se

Abstract

Today, Li-ion batteries (LIBs) play a vital role in reducing the consumption of fossil fuels. With the increasing production of LIBs, it is crucial to consider their recycling after reaching their end-of-life. Pyrometallurgy is a technique that can be employed for the recycling of LIBs, which deals with the formation of three phases: melt, slag, and gas. In-situ alloying by the addition of hematite to the LIB black mass was studied previously by the authors. The effect of slag composition in terms of $CaO:SiO_2$ ratio on the aforementioned system in terms of the melting, slag/metal separation, and Li/F evaporation behavior has been investigated in this work. The $CaO:SiO_2$ mass ratios of 0:100, 25:75, 50:50, 75:25, and 100:0 were tested in that system at a temperature of 1450 °C. Thermodynamic modeling with FactSage 8.0 supported the experimental work. From this qualitative study, it can be anticipated that by increasing the SiO_2 amount, metallics coalesce more effectively, the probability of metal/slag separation increases, and Li evaporation is enhanced. The addition of CaO may result in the entrapment of Li within the Ca silicate structure and decrease its vapor partial pressure. Thermodynamic modeling revealed a consistent trend in the distribution of Li and F as the $CaO:SiO_2$ ratio changed, suggesting the potential formation of gaseous compounds such as LiF.

Keywords: Lithium-ion battery, pyrometallurgy, recycling, slag, in-situ alloying

1.   INTRODUCTION

In recent years, attention has been drawn to decreasing the consumption of fossil energies and instead replacing them with renewable energies. This goal cannot be achieved unless rechargeable batteries are employed to store these energies. Li-ion batteries (LIBs) are one of the popular candidates among rechargeable batteries with remarkable properties [1-4]. It has been predicted that the amount of LIB waste will increase drastically in the upcoming years, while in 2020 less than 5 % of them were recycled. Following that, the EU directive regulated that 65 % of Li-based batteries should be recycled by 2025, and this rate should reach 70 % by 2030, aiming at achieving a recovery rate of 90 % for Co, Cu, and Ni, and 50 % recovery rate for Li by 2027 [5-7]. The materials used in the LIB cells are approximately 50 % of the whole LIB composition, which costs about 50 % of the battery manufacturing total costs [8-10]. Hence, it is required to establish environment-friendly methods to recover the precious elements in the LIBs. After applying a series of pretreatments on the battery cell, a black powder, called black mass (BM), is obtained. BM is rich in cathode and anode active materials, mainly Li metal oxides and graphite.

Pyrometallurgy is a technique that can be employed for recovering precious elements in the BM, which in case of employing high temperatures (higher than 1400 °C), deals with melting the BM. To enhance the separation of different elements, fluxes can be added to form a slag phase. One of the challenging elements to recover in the BM is Li. Concerning Li, the goal can be either Li slagging or Li evaporation [9], [11-13].

A method for recovering Co and Ni from Black Mass (BM, obtained from LIBs) was studied before by the authors, where an Fe-based alloy was formed by adding hematite to the BM [14]. Following that, the effect of the CaO-SiO$_2$ slag system on the alloying process has been qualitatively studied in this work.

2.   EXPERIMENTAL

Two types of BM obtained from two types of LIBs (LCO and NMC111, called NMC hereafter) were used in this study, the composition of which is available in the reference [14]. Hematite (-325 mesh, 98 %, Alfa Aesar) was added to these two BM types, achieving a total C/O molar ratio of one. CaO (in the form of CaCO$_3$, 5 μm, 99.5 %, Alfa Aesar) and SiO$_2$ (-325 mesh, 99.5 %, Alfa Aesar) were added as fluxes to the hematite+BM mixtures with the CaO+SiO$_2$/hematite+BM mass ratio of 1:3. The composition of the added flux (CaO:SiO$_2$) was in the ratios of 0:100, 25:75, 50:50, 75:25, and 100:0 g:g. The mixtures were placed in MgO crucibles and heated up to 1450 °C (with a rate of 10 °C/min) and then held at that temperature for 60 min in a Netzsch STA 409 ThermoGravimetric Analyzer (TGA) with a detection limit of ±1 μg. The experiments were run under Ar atmosphere with a flow rate of 100 mL/min. Inductively Coupled Plasma Atomic Emission Spectroscopy (ICP-OES), ThermoScientific iCAP 7200, was used to analyze the samples after the heat treatment. Thermodynamic modeling with FactSageTM 8.0 was done supporting the experimental work.

3.   RESULTS AND DISCUSSION

Figure 1 represents the crucibles containing hematite+BM mixtures with different ratios of CaO:SiO$_2$, after heating up to 1450 °C. Monitoring the crucible images reveals that by decreasing the amount of SiO$_2$, the probability of metal/slag separation decreases, and the system gradually alters to a solid system. Moreover, it should be noted that increased SiO$_2$ in the system results in metallic droplets coalescing and therefore enhances slag metal separation.
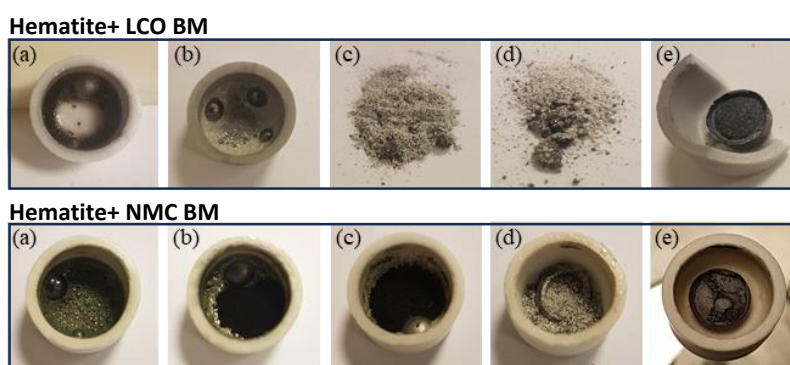

Figure 1 Samples obtained from heating the hematite+BM+slag mixtures at 1450 °C: CaO:SiO$_2$ ratios of (a) 0:100, (b) 25:75, (c) 50:50, (d) 75:25, and (e) 100:0 g:g

The TGA graphs of these samples in **Figure 2** also show that the main mass loss occurs at a temperature lower than 1000 °C, and the slope changes afterward.
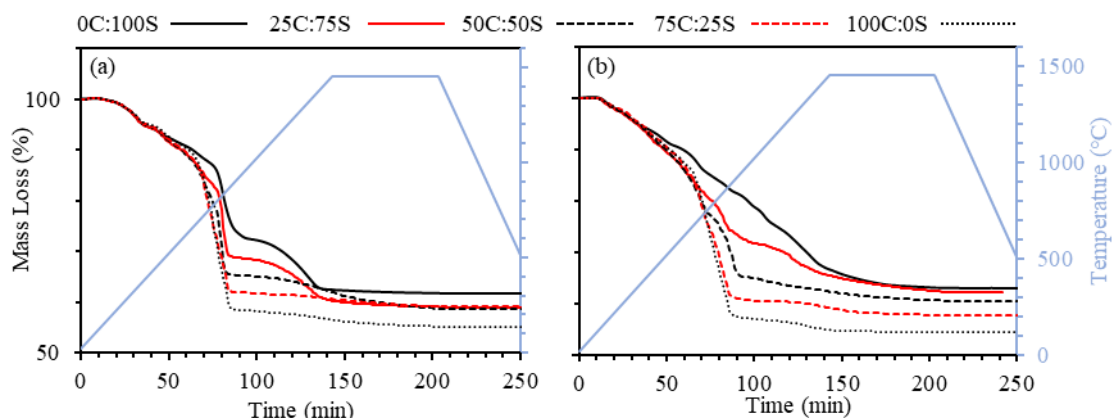
Figure 2 Effect of slag formers composition on thermal behaviour of hematite+BM mixtures in two types of (a) LCO, and (b)NMC

In order to have a better understanding of the mass loss, the net mass loss has been normalized by discarding excess CO_2 in $CaCO_3$ (see **Table 1** and **Table 2**).

Table 1 Calculation on discarding the effect of excess CO_2 in $CaCO_3$ in hematite+LCO mixtures

CaO:SiO$_2$	Net mass loss (Experimental)	Net mass loss (Normalized)
0:100	38.4	38.4
25:75	41.1	38.2
50:50	41.5	35.9
75:25	41.0	32.4
100:0	44.9	34.0

Table 2 Calculation on discarding the effect of excess CO_2 in $CaCO_3$ in hematite+NMC mixtures

CaO:SiO$_2$	Net mass loss (Experimental)	Net mass loss (Normalized)
0:100	37.1	37.1
25:75	37.8	34.8
50:50	39.5	33.7
75:25	42.3	33.9
100:0	45.5	34.8

Attempts were made to separate the slag and metal phases by magnetic separation or manual separation of metallic droplets from the slag matrix. In some cases, it was not possible to separate them using simple applied methods. Separated fractions or the whole sample (in case of failed separation) were further analyzed by ICP-OES. The chemical analysis of the main elements, including Li, was used to perform a qualitative mass balance; the contents were normalized based on the Fe content. The results of the hematite-LCO mixture are presented in **Figure 3**. **Figure 3** (a-e) shows the compositions by increasing the CaO:SiO$_2$ ratio and **Figure 3**-f is for the sample without the addition of slag formers. To better distinguish the Li changes, the chart is magnified in each diagram. Although Fe and Co show almost similar behavior in all cases, Li behaves differently. The results show that the Li content in the condensed phase approaches zero, i.e., most of the Li is distributed in the gas phase. The ICP results for the divided samples show that Li in the condensed phase is mostly present in the non-magnetic phase (probably slag), and, by increasing the CaO:SiO$_2$ ratio, Li increases in this phase. The chemical composition of hematite+NMC samples after reduction (**Figure 4**) shows that, as expected, Co and Ni (together with Fe) accumulate in the metallic/magnetic part. It seems that the

increase in the CaO:SiO$_2$ ratio hinders Mn solubility in the slag and increases the Mn dissolution in the alloy matrix.
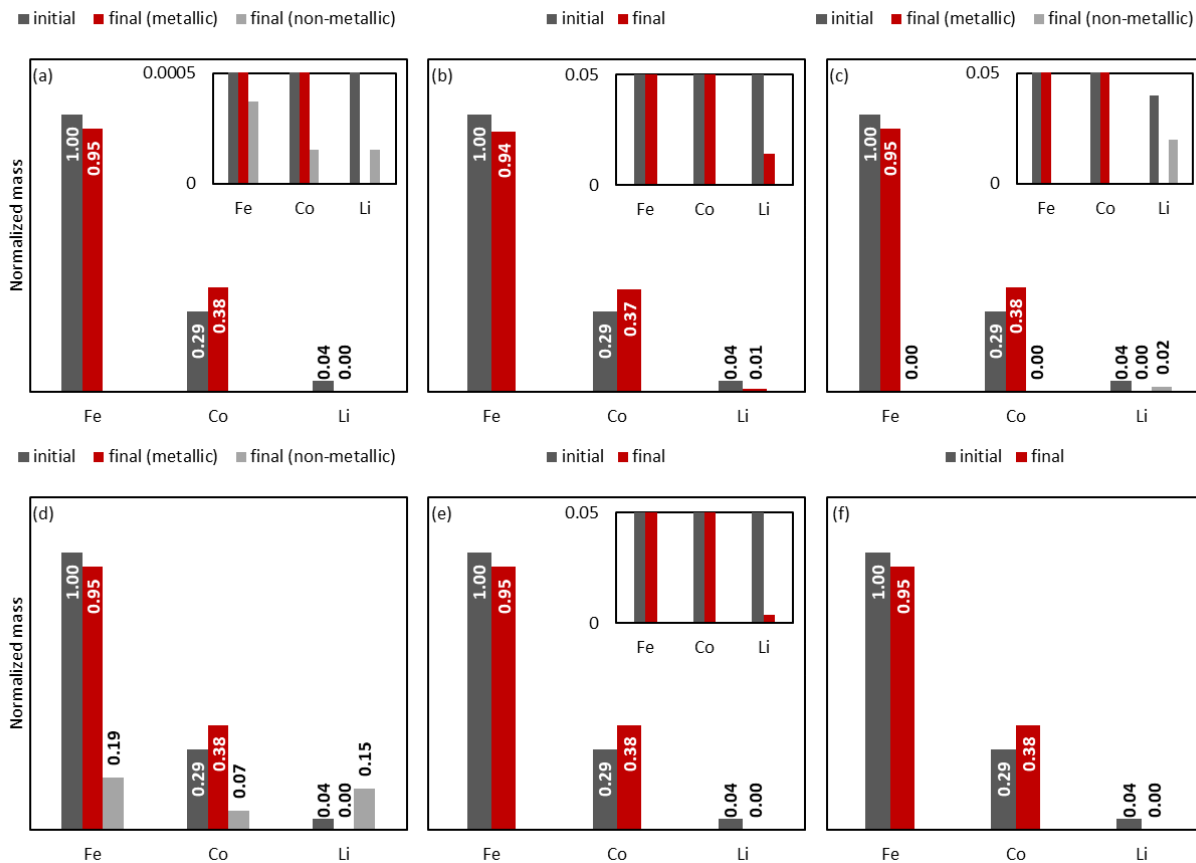

Figure 3 Effect of slag formers composition on the chemical composition of hematite+LCO mixture with the different slag former ratios of (a) 0:100, (b) 25:75, (c) 50:50, (d) 75:25, (e) 100:0 g:g CaO:SiO$_2$, and (f) without slag former.
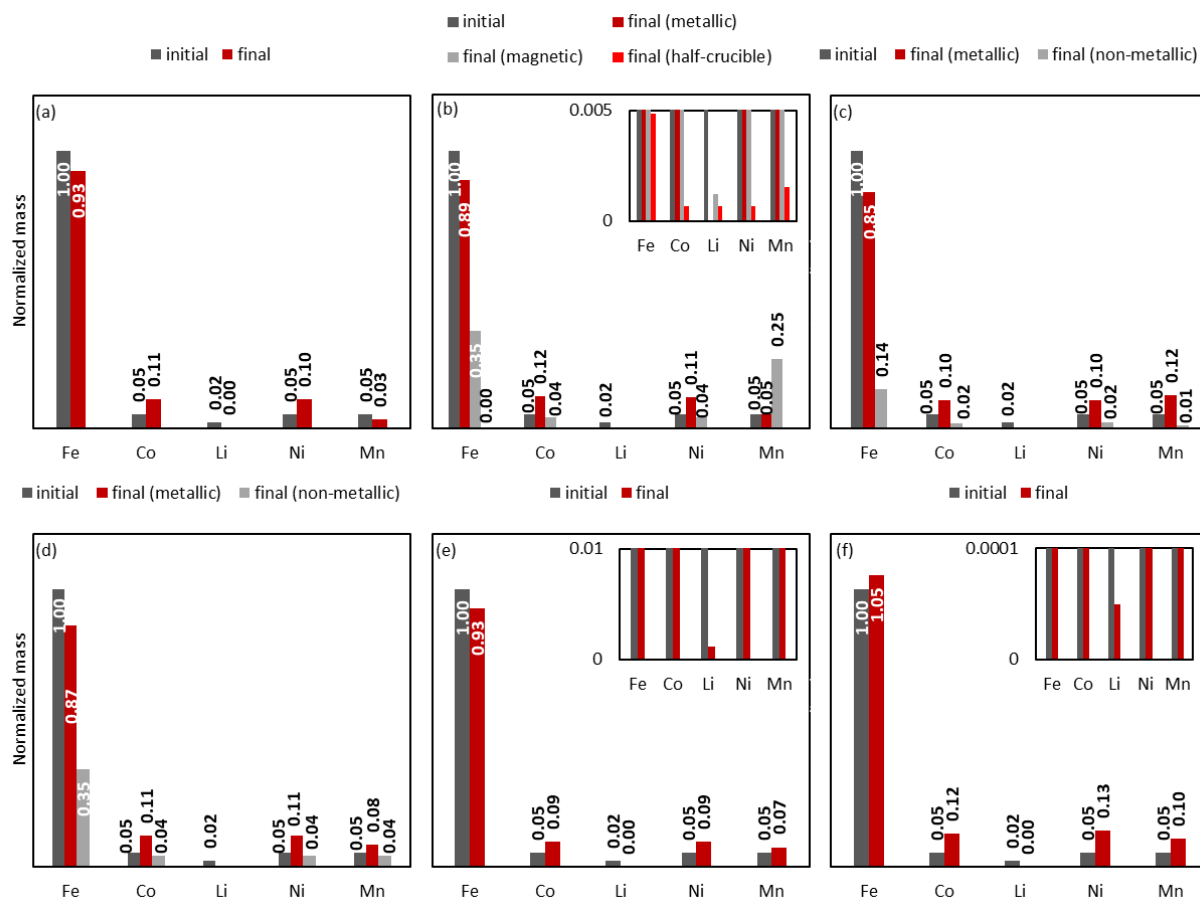
Figure 4 Effect of slag formers composition on the chemical composition of hematite+NMC mixture with the different slag former ratios of (a) 0:100, (b) 25:75, (c) 50:50, (d) 75:25, (e) 100:0 g:g $CaO:SiO_2$, and (f) without slag former.

It was observed (**Figure 1**) that the addition of CaO makes the metal/slag separation difficult, and the metallics do not coalesce as effectively as they did with higher SiO_2 content. The first drop in the TGA graphs (**Figure 2**) originates from the main reduction of BM and hematite, followed by a steady decline that seems to be related to the Fe melting at about 800 °C (calculated by FactSage). The mass loss was slightly higher in the systems containing only SiO_2 or CaO, which can be due to Li evaporation based on the chemical analysis and thermodynamic modeling. It is likely that the formation of Ca silicates entraps Li in the slag and prevents its evaporation.

Thermodynamic calculations (**Figure 5**) demonstrate that increasing the CaO leads to the formation of a solid monoxide phase. In FactSage, the monoxide phase is representative of FeO, CaO, MgO, SrO, BaO, MnO, NiO, CoO at all compositions together with Al,Fe(III), Cr(III), Li, Na, Ti(IV), Zn, Zr in dilute amounts. In the NMC case, 100 % SiO_2 leads to oversaturation and formation of solid SiO_2.
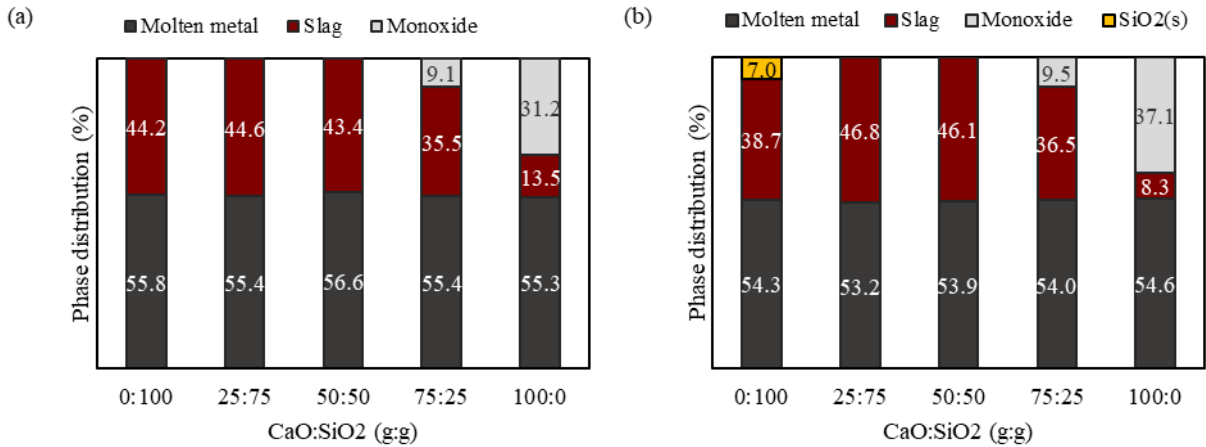
Figure 5 Effect of slag composition on the distribution of condensed phases in the mixture of hematite with (a) LCO, and (b) NMC at 1450 ℃, calculated by FactSage.

The Li phase distribution, calculated by FactSage, is depicted in **Figure 6**. The figure shows that Li is mainly dissolved in the slag phase. It can also be seen that more Li is accumulated in the gas phase in the case of 100 % CaO, and that the same content is maintained in the range of 25-75 % CaO. This range of $CaO:SiO_2$ ratio is close to the basicity range used for industry slags. Comparing the phase distribution trend of Li with the F distribution (**Figure 7**), they behave similarly, which can prove their presence in the same compounds, e.g., LiF.
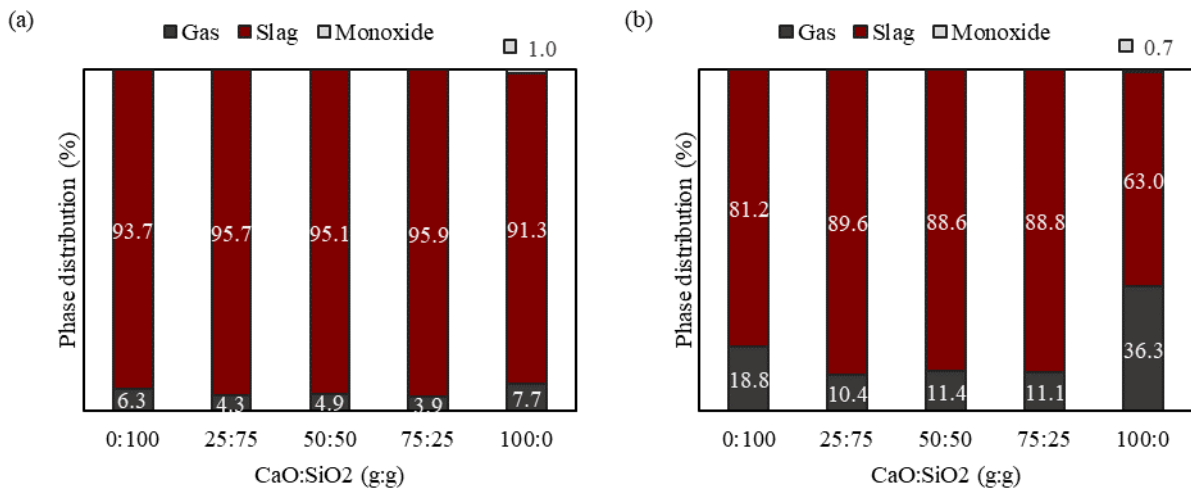

Figure 6 Effect of slag composition on the Li distribution in the mixture of hematite with (a) LCO, and (b) NMC at 1450 ℃, calculated by FactSage.
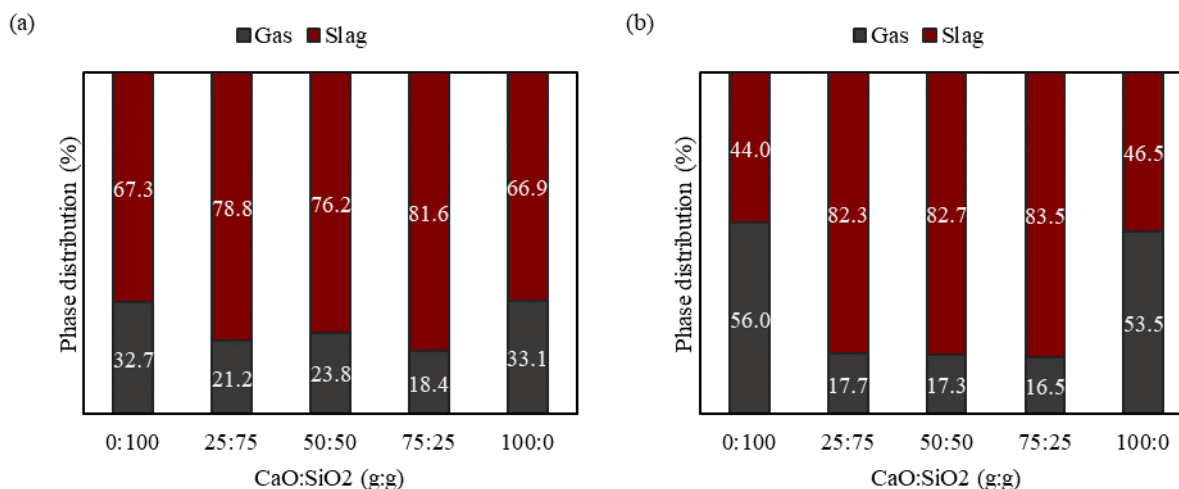
Figure 7 Effect of slag composition on the F distribution in the mixture of hematite with (a) LCO, and (b) NMC at 1450 ℃, calculated by FactSage.

Finally, it should be mentioned that further studies are required on the effect of slag on Li evaporation in the discussed system, which will be the focus of the authors' future research.

4. CONCLUSION

With an aim to suggest a sustainable pyrometallurgical method for recycling LIBs' BM, the effect of slag composition in terms of $CaO:SiO_2$ ratio on the melting, slag/metal separation, and Li/F evaporation behavior was qualitatively investigated, considering the thermodynamics of the system. Different compositions of CaO-SiO_2 slag were studied in a system containing hematite and BM and it was observed that metallics better coalesce in a lower $CaO:SiO_2$ ratio. Better Li evaporation is possibly expected in lower $CaO:SiO_2$ ratio and, by addition of CaO, the entrapment of Li in the Ca silicate structure is likely to occur. Thermodynamic calculations show a similar trend for Li and F distribution with changing the $CaO:SiO_2$ ratio, which can be a hint for the formation of gaseous compounds containing Li and F like LiF.

REFERENCES

[1] ARMAROLI, N., BALZANI V. *Towards an electricity-powered world*. [online] 2011 [viewed: 2024-05-20]. Available from: http://xlink.rsc.org/?DOI=c1ee01249e

[2] ZENG, X., LI, J., LIU, L. *Solving spent lithium-ion battery problems in China: Opportunities and challenges*. [online] 2015 [viewed: 2024-05-20]. Available from: https://linkinghub.elsevier.com/retrieve/pii/S136403211500859X

[3] ZHENG, X., ZHU, Z., LIN, X., ZHANG, Y., HE, Y., CAO, H., SUN, Z. *A mini-review on metal recycling from spent lithium ion batteries*. [online] 2018 [viewed: 2024-05-20]. https://doi.org/10.1016/j.eng.2018.05.018

[4] ZHANG, W., XU, C., HE, W., LI, G., HUANG, J. *A review on management of spent lithium ion batteries and strategy for resource recycling of all components from them*. [online] 2018 [viewed: 2024-05-20]. Available from: http://journals.sagepub.com/doi/10.1177/0734242X17744655

[5] KING, S., BOXALL, N.J. *Lithium battery recycling in Australia: defining the status and identifying opportunities for the development of a new industry*. [online] 2019 [viewed: 2024-05-20]. Available from: https://doi.org/10.1016/j.jclepro.2019.01.178

[6] LIANG, Y., ZHAO, C.Z., YUAN, H., CHEN, Y., ZHANG, W., HUANG, J.Q., YU, D., LIU, Y., TITIRICI, M.M., CHUEH, Y.L., YU, H., ZHANG, Q. *A review of rechargeable batteries for portable electronic devices*. [online] 2019 [viewed: 2024-05-20]. Available from: https://doi.org/10.1002/inf2.12000

[7] EUROPEAN PARLIAMENT AND THE COUNCIL OF THE EUROPEAN UNION. *Regulation (EU) 2023/1542 of the European Parliament and of the Council of 12 July 2023 concerning batteries and waste batteries, amending Directive 2008/98/EC and Regulation (EU) 2019/1020 and repealing Directive 2006/66/EC*. [online] 2023 [viewed: 2024-05-20]. Available from: http://data.europa.eu/eli/reg/2023/1542/oj

[8] PISTOIA, G. *Lithium-ion batteries advances and applications*. Amsterdam: Elsevier, 2014.

[9] HARPER, G., SOMMERVILLE, R., KENDRICK, E., DRISCOLL, L., SLATER, P., STOLKIN, R., WALTON, A., CHRISTENSEN, P., HEIDRICH, O., LAMBERT, S., ABBOTT, A., RYDER, K., GAINES, L., ANDERSON, P. *Recycling lithium-ion batteries from electric vehicles*. [online] 2019 [viewed: 2024-05-20]. Available from: http://dx.doi.org/10.1038/s41586-019-1682-5

[10] TRÄGER, T., FRIEDRICH, B., WEYHE, R., TRA, T. Recovery concept of value metals from automotive lithium-ion batteries. [online] 2015 [viewed: 2024-05-20]. Available from: https://doi.org/10.1002/cite.201500066

[11] MAKUZA, B., TIAN, Q., GUO, X., CHATTOPADHYAY, K., YU, D. *Pyrometallurgical options for recycling spent lithium-ion batteries: A comprehensive review*. [online] 2021 [viewed: 2024-05-20]. Available from: https://doi.org/10.1016/j.jpowsour.2021.229622

[12] KLIMKO, J., ORÁČ, D., MIŠKUFOVÁ, A., VONDERSTEIN, C., DERTMANN, C., SOMMERFELD, M., FRIEDRICH, B., HAVLÍK, T. A. *Combined pyro- and hydrometallurgical approach to recycle pyrolyzed lithium-ion battery black mass part 2: Lithium recovery from Li Enriched slag—thermodynamic study, kinetic study, and dry digestion*. [online] 2020 [viewed: 2024-05-20]. Available from: https://www.mdpi.com/2075-4701/10/11/1558

[13] QU, G., WEI, Y., LIU, C., YAO, S., ZHOU, S., LI, B. *Efficient separation and recovery of lithium through volatilization in the recycling process of spent lithium-ion batteries*. [online] 2022 [viewed: 2024-05-20]. Available from: https://doi.org/10.1016/j.wasman.2022.06.039

[14] BABANEJAD, S., AHMED, H., ANDERSSON, C., HEIKKINEN, E.P. *Mechanical activation-assisted recovery of valuable metals from black mass in the form of Fe/Cu alloys*. [online] 2023 [viewed: 2024-05-20]. Available from: https://link.springer.com/10.1007/s40831-023-00665-6